Preparation of Pd–B/palygorskite amorphous catalyst for the selective hydrogenation of *o*-chloronitrobenzene to *o*-chloroaniline

Mei Wu[1,3], Ying Xu[3], Jinlong Jang[1,2,3] ✉, Jingxi Ju[1], Qingyun Zeng[4], Chuansong Duanmu[3], Xu Gu[3]

[1]*Zhejiang Province Key Laboratory of Noble Metal Catalytic Materials and Technology, Hangzhou 310015, People's Republic of China*
[2]*Faculty of Chemical Engineering, Key Laboratory for Palygorskite Science and Applied Technology of Jiangsu Province, Huaiyin Institute of Technology, Huaian 223003, People's Republic of China*
[3]*Jiangsu Provincial Engineering Laboratory for Advanced Materials of Salt Chemical Industry, Huaiyin Institute of Technology, Huaian 223003, People's Republic of China*
[4]*Beijing Research Institute of Uranium Geology, Beijing 100029, People's Republic of China*
✉ *E-mail: jiangjinlong75@163.com*

Pd–B amorphous alloy was successfully supported on the surface of natural nanoclay palygorskite (PAL) via a simple chemical reduction method. Compared with the conventional supported Pd catalyst, the Pd–B/PAL amorphous catalyst possessed the ultra-high selectivity (100%) to *o*-chloroaniline (*o*-CAN) in the hydrogenation of *o*-chloronitrobenzene (*o*-CNB) to *o*-CAN and avoided the dechlorination of *o*-CNB. XPS analysis results indicated that PAL support could reduce the electron density of Pd atoms and suppressed the hydrogenolysis of C–Cl bond. Meanwhile, the Pd–B/PAL amorphous catalyst exhibited a good stability and is a prospective catalyst for the selective hydrogenation of CNB to CAN.

1. Introduction: Chloroaniline (CAN) is an important intermediate in the manufacture of drugs, pesticides, dyes, and herbicides. CAN is generally prepared by the reduction of chloronitrobenzene (CNB) in a metal-acid system. However, the traditional synthetic routes of CAN are harmful to the environment. Catalytic hydrogenation of CNB to the corresponding CAN has attracted much attention due to its atomic economy and environment-friendly process [1–4]. In a hydrogenation process, hydrodechlorination reaction often occurred, resulting in a low selectivity to CAN [2–4]. To overcome this problem, many strategies have been developed to improve the selectivity to CAN, such as adjusting the properties of catalyst (active metal, metal particles size, and support), optimising the reaction conditions (temperature, solvent etc), or introducing some additives (promoter, inhibitor, and poison) [1–11]. Compared with other metal catalysts, precious metal platinum exhibits an excellent catalytic performance and higher selectivity in the hydrogenation process. For example, Pt/γ-Fe$_2$O$_3$ could completely convert *o*-CNB to *o*-CAN with 100% selectivity to *o*-CAN [12]. Small amount of platinum also could promote the catalytic activity of Au/TiO$_2$ catalyst in hydrogenation of *p*-CNB to reach 100% selectivity to *p*-CAN [13]. An HCl-acidified palygorskite (PAL) supported platinum catalyst also exhibited an excellent activity and 100% selectivity in the chemoselective hydrogenation of CNB to CAN [14]. HCl-acidified PAL support might suppress the hydrodechlorination due to its special structure and components. The results indicated that the supports of the catalysts played a crucial role in the selective hydrogenation of CNB.

Palladium is another frequently-used precious metal catalyst with high catalytic activity for hydrogenation of CNB to the corresponding CAN [11, 15, 16]. Although compared with platinum, it is low-cost, the hydrodechlorination reaction over the supported Pd catalysts is hard to avoid, resulting in a relative low selectivity to CAN [15]. Some efforts have been attempted to suppress the hydrodechlorination over the supported Pd catalysts, such as the modification of Sn^{4+} [11] and diphenyl sulphide to Pd [16], and the combination of Pd and Au [2]. Those strategies all exhibited high selectivity to CAN, however, the supported Pd catalysts with an excellent performance is still a challenge.

Pd–B amorphous alloy is a hydrogenation catalyst with a long-range disordered but short-range ordered structure and exhibits an excellent catalytic activity in the hydrogenation of nitro compound and tricyclopentadiene [17–19]. The introduction of B into Pd could improve the catalytic performance of the catalyst and suppress the dechlorination for its special amorphous structure and charge effect [20]. The 99.9% conversion yield and 98% selectivity in the hydrogenation of *o*-CNB to *o*-CAN over a Pd–B/Al$_2$O$_3$ amorphous alloy catalyst have been obtained [20]. Both the nature of the supported amorphous metal and the structure of the Al$_2$O$_3$ support affected the hydrogenation performance of *o*-CNB.

PAL is a kind of natural clay mineral and has attracted much attention for its application in the catalyst supports [14, 21–23]. The combination of the active component and PAL remarkably enhanced the catalytic performance of the composite catalyst [14, 23]. In this Letter, Pd–B amorphous alloy was supported on PAL fibres by the chemical reduction with NaBH$_4$. The catalytic performance of Pd–B/PAL amorphous catalyst for the hydrogenation of *o*-CNB was investigated.

2. Experimental
2.1. Preparation of catalysts: Purified PAL (1 g) was mixed with 10 ml PdCl$_2$ aqueous solution and sonicated for 30 min resulting in a suspension, which was further magnetically stirred for 2 h at room temperature. The NaBH$_4$ solution (20 ml/l) was added dropwise into the suspension until bubbles were not observed in the resulting solution. The Pd–B/PAL catalysts were filtrated, washed with distilled water, and dried at 60°C for 12 h under vacuum. To investigate the influence of Pd content on the catalytic properties of the catalyst, the PdCl$_2$ concentration were selected as 0.83, 1.67, and 4.99 g/l, and the Pd content of the obtained catalysts were 0.5, 1, and 3 wt%, respectively. The corresponding catalysts were denoted as 0.5, 1, and 3% Pd–B/PAL, respectively. For comparison, Pd/PAL catalyst with 1 wt% Pd (denoted as 1%Pd/PAL) was prepared by an impregnation-reduction method. The reduction temperature and time was 300°C and 2 h.

2.2. Catalyst characterisation: X-ray diffraction (XRD) patterns were performed on a Bruker D8 Discover X-ray diffractmeter

with a Cu Kα source at 40 mV and 40 mA. Transmission electron microscope measurements (TEM) were carried out in a FEI Tecnai G20 instrument at an accelerating voltage of 200 kV. The scanning electron microscopy images were obtained on an FEI Quanta FEG250 microscope. The chemical status of Pd in the catalysts was determined by X-ray photoelectron spectroscopy (XPS, Thermo ESCALAB 250XI). The contents of palladium and boron elements in the catalysts were measured on a Perkin-Elmer Optima 7000DV (inductively coupled plasma-atomic emission spectrometry (ICP-AES)) instrument.

2.3. Catalytic evaluation: The catalytic hydrogenation of o-CNB was carried out in a 50 ml stainless steel autoclave with a thermocouple and a magnetic stirring bar. In a typical reaction procedure, 0.1 g o-CNB and 0.02 g catalyst were mixed with 10 ml ethanol in the autoclave, which was then purged with H_2 for three times and pressurised to 1 MPa. The reaction mixture was heated to 40°C and kept for 40 min, before it was cooled down to the room temperature and slowly depressurised. The catalyst was separated from the reaction liquid by centrifugation. The liquid mixture was analysed by an Agilent 6820 gas chromatograph with a hydrogen flame ionisation detector (FID) and a DB-1 column. For recycling experiments, the catalyst was separated from the reaction mixture, washed with ethanol and then redispersed in 10 ml ethanol.

3. Results and discussion

3.1. Characterisation of Pd–B/PAL catalyst: Fig. 1 shows the XRD curves of PAL and the prepared Pd–B/PAL catalysts with different Pd contents. As shown in Fig. 1a, the diffraction peaks at 8.3°, 19.7°, and 27.3° could be identified from PAL [21, 22]. In addition, a weak diffraction peak at 26.5° was attributed to quartz [22], which was coexisted with PAL in the mineral with a very low content. No obvious diffraction peaks ascribed to Pd were observed from the XRD curves of Pd–B/PAL catalysts in Fig. 1a. However, the magnified XRD curves of Pd–B/PAL catalysts (Fig. 1b) exhibited a weak broad diffraction peak at 40° (signed by black arrow), which was the characteristic of amorphous Pd [19]. The intensity of the characteristic peak also increased with the Pd content. The results indicated that Pd–B amorphous alloy was successfully loaded on the PAL fibres.

Fig. 2 shows TEM images of PAL and 1%Pd–B/PAL catalyst. As shown in Fig. 2a, PAL was fibrous crystals with smooth surface and the diameter was in a range of 20–80 nm. PAL remained the fibrous morphology and the nanoparticles with the size of 12 nm appeared on the surface of PAL crystals after Pd–B amorphous alloy loading (Fig. 2b). The interactions between metal nanoparticles and –OHs group at the surface of PAL crystals could promote nanoparticles to deposit on PAL fibres [21]. Hence, Pd–B nanoparticles were highly dispersed and attached on the support PAL crystals. The results further confirmed the existence of Pd–B amorphous alloy in the 1%Pd–B/PAL catalyst and were in good agreement with the XRD data.
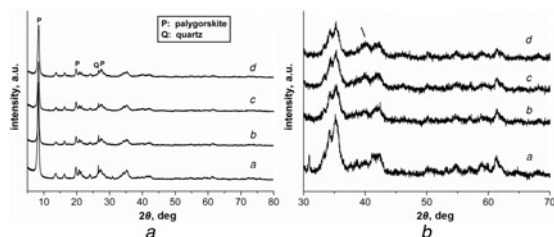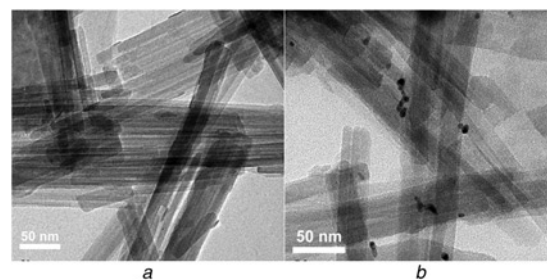

Fig. 2 *TEM images*
a PAL
b 1%Pd–B/PAL catalyst

Fig. 3 displays the XPS spectra of Pd 3d for Pd–B/PAL catalyst with 1 and 3 wt% Pd, respectively. For the 1%Pd–B/PAL catalyst, two peaks with binding energy at 336.1 eV (Pd $3d_{5/2}$) and 338.4 eV (Pd $3d_{3/2}$) could be observed in Fig. 3a, which could be assigned to Pd^0 and Pd^{2+}, respectively, according to previous reports from Luo *et al.* [20] and Hou and Yang [23]. Obviously, Pd in the Pd–B/PAL catalyst was mainly at +2 valence state. The atomic ratio of Pd^0/Pd^{2+} was about 0.5. The results indicated that Pd^{2+} ions were partially reduced to Pd^0 by $NaBH_4$ in the Pd–B/PAL catalyst, which might be caused by the exchange of Pd^{2+} with Mg^{2+} and Al^{3+} of PAL [21]. As shown in Fig. 3b, the Pd spectra of the Pd–B/PAL catalyst contained three peaks with binding energy at 335.3, 337.8, and 340.3 eV, when the Pd content increased to 3 wt%. The peak at 337.8 eV was assigned to Pd^{2+} [23], while another two peaks were attributed to the electron transitions of $3d_{5/2}$ and $3d_{3/2}$ of Pd^0 [19]. Obviously, zero-valent Pd was the primarily valance state of Pd in the 3%Pd–B/PAL catalyst, and the atomic ratio of Pd^0/Pd^{2+} increased to 5.1. The result might be caused by the limited ion exchange capacity of PAL. Pd^{2+} ions were continually reduced to zero-valent Pd species with the increase of Pd content when the exchange capacity of PAL for Pd^{2+} ions reached to saturation. We also investigated the XPS spectra of 1%Pd/PAL catalyst (shown in Fig. 3c). The results were similar to that of 1%Pd–B/PAL catalyst except that the bind energy of Pd species decreased slightly. The results indicated that Pd species with +2 valence state was the primary Pd species in 1%Pd/PAL catalyst. The results further confirmed that Pd^{2+} ions exchanged with Mg^{2+} and Al^{3+} of PAL in the preparation process of catalyst, which avoided the reduction completely of Pd^{2+}
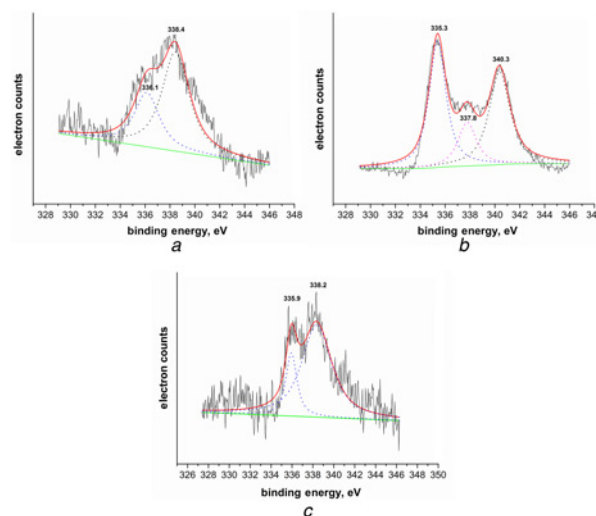

Fig. 1 *XRD patterns of PAL (a) and Pd–B/PAL catalysts with 0.5 (b), 1 (c), and 3 (d) wt% Pd*
a XRD curves
b Magnified XRD curves

Fig. 3 *XPS spectra of Pd3d*
a 1%Pd–B/PAL
b 3%Pd–B/PAL
c 1%Pd/PAL

Table 1 Pd and B content of Pd-B/PAL catalyst[a]

Catalysts	Pd, wt%	B, wt%
0.5%Pd–B/PAL	0.42	0.62
1%Pd–B/PAL	0.97	1.37
3%Pd–B/PAL	2.86	1.96
Recycled 1%Pd-B/PAL[b]	0.21	0.81

[a]Determined by ICP.
[b]Recycling times: 5.

ions under hydrogen atmosphere. In addition, it was noted that the binding energy of Pd species in the Pd–B/PAL catalyst all shifted positively compared with the standard binding energy of Pd^0 (335 eV) and Pd^{2+} (337.5 eV). The results meant that the electron density of Pd atoms decreased despite the electron transfer from B to Pd [17]. PAL contains a large amount of acid sites [24]. Therefore, the results might be caused by the electron adsorption of the acid cites of PAL supports from Pd atoms. On the other hand, the increase of the binding energy of Pd species became smaller for the limited acid cites of PAL when the Pd content in the Pd–B/PAL catalyst increased. The phenomenon resulted in the electronic shortage of Pd atoms and was also beneficial to improve the hydrogenation selectivity of the catalyst [25].

Table 1 shows the Pd and B contents in three differently prepared Pd–B/PAL amorphous catalysts. It can be seen that the catalysts all contained Pd and B elements, further indicating that the catalytic active component supported on the PAL was Pd–B amorphous alloy. The real Pd content was 0.42, 0.97, and 2.86 wt% and slightly below to the desired Pd content.

3.2. Catalytic performance of Pd–B/PAL catalyst: Reaction temperature is an important factor influencing the catalytic performance in the hydrogenation reaction. Generally speaking, high reaction temperature could enhance the hydrogenation reaction rate, but also limit the chemoselectivity [20]. Thus, the reaction temperature was controlled at the range of 30–100°C to investigate the effect of the temperature on the catalytic properties of the catalyst. Table 2 shows the effect of reaction temperature on the catalytic hydrogenation performance of o-CNB over the 1%

Pd–B/PAL catalyst. It can be seen that the conversion of o-CNB was only 30.87% when the reaction temperature was at 30°C. However, Pd–B/PAL catalyst exhibited excellent hydrogenation activity and selectivity for the selective hydrogenation of o-CNB when the reaction temperature increased to the range of 40–100°C. Both the conversion of o-CNB and selectivity to o-CAN reached to 100%. No dechlorination product was found in the reaction mixture. The excellent hydrogenation activity and selectivity of Pd–B/PAL catalyst was also kept even though the Pd content increased from 0.97 to 2.86 wt%. The results indicated that the Pd-B/PAL catalyst possess an excellent hydrogenation activity and ultra-high selectivity for the catalytic hydrogenation of o-CNB.

The effect of reaction time on the catalytic performance of the Pd–B/PAL catalyst was also investigated when the reaction temperature was at 40°C and the corresponding results are listed in Table 2. For the 1%Pd–B/PAL catalyst, the conversion of o-CNB and selectivity to o-CAN all reached 100% when the reaction time was 0.5 h. The similar results were also obtained when 0.5%Pd–B/PAL catalyst with a relatively low Pd content (0.42 wt %) was used as the hydrogenation catalyst. The results further illustrated that the Pd–B/PAL catalyst possess an excellent hydrogenation activity and selectively for the catalytic hydrogenation of o-CNB.

The Pd–B/PAL catalysts also exhibited an excellent catalytic performance and selectivity for the catalytic hydrogenation of o-CNB when Pd content was in the range of 0.42–2.86 wt%. However, the conversion of o-CNB over 1%Pd–B/PAL catalyst was only 75.87% at 40°C when the dosage of substrate o-CNB was increased to 0.5 g, indicating that the turnover frequency (TOF) of Pd–B/PAL catalyst was $1320.57 h^{-1}$. The effect of PAL on the catalytic performance of Pd–B/PAL catalyst was also investigated. Interestingly, 1%Pd/PAL catalyst prepared by the impregnation-reduction method also exhibited similar catalytic performance and selectivity (100%) compared with Pd–B/PAL catalyst. B atoms could increase the electron density of Pd atoms through the electron transfer, which was beneficial to the adsorption of o-CNB on the catalyst, resulting in the increase of the activity of catalyst [17]. Luo et al. [20] reported that the selectivity of o-CAN over Pd–B/Al$_2$O$_3$ catalyst was 98%, indicating that Pd–B amorphous catalyst did not completely avoid the dechlorination of o-CNB. Ma et al. [14] reported that that the special structure and components of PAL might suppress the

Table 2 Catalytic results of the catalytic hydrogenation of o-CNB over the Pd–B/PAL catalysts and Pd/PAL catalyst[a]

Catalysts	$m_{o\text{-CNB}}$, g	Temperature, °C	Time, h	Conversion, %[b]	$S_{o\text{-CAN}}$, %[c]
1%Pd–B/PAL	0.1	30	2.0	30.87	100
	0.1	40	2.0	100	100
	0.1	50	2.0	100	100
	0.1	60	2.0	100	100
	0.1	40	0.5	100	100
	0.1	40	1.0	100	100
	0.1	40	1.5	100	100
	0.3	40	1	100	100
	0.5	40	1	75.87	100
0.5%Pd–B/PAL	0.1	40	0.5	100	100
	0.1	40	1	100	100
	0.1	40	1.5	100	100
	0.1	40	2	100	100
3%Pd–B/PAL	0.1	40	2	100	100
	0.1	50	2	100	100
	0.1	80	2	100	100
	0.1	100	2	100	100
1%Pd/PAL	0.1	40	2	100	100

[a]Reaction conditions: Pd–B/PAL catalyst 0.02 g, ethyl alcohol 10 mL, 1.0 MPa H$_2$.
[b]Conversion of o-CNB was determined by gas chromatography (GC).
[c]Selectivity to o-CAN was determined by GC.

Table 3 Recycling of the 1%Pd–B/PAL catalyst[a]

Recycling time	o-CNB conversion, %[b]	o-CAN selectivity, %[b]
1	100	100
2	100	100
3	100	100
4	80.21	100
5	0	0

[a]Reaction conditions: Pd–B/PAL catalyst 0.02 g, o-CNB 0.1 g, ethyl alcohol 10 ml, 40°C, 1.0 MPa H_2, and 120 min.
[b]Determined by GC.

hydrodechlorination of o-CNB and result in ultra-high selectivity of o-CAN. Our results further confirmed the phenomenon. Pd atoms in the Pd–B/PAL catalyst might easily adsorb the negative oxygen atoms of nitro groups for their low electron density, which could suppress the hydrogenolysis of C–Cl bond and improve the selectivity of o-CAN.

3.3. Stability of Pd–B/PAL catalyst: The reusability test of Pd–B/PAL catalyst was carried out under the same reaction condition. After each reaction, the used catalyst was filtered, washed with ethyl alcohol, and then applied to the next hydrogenation reaction. The results are listed in Table 3. The activity of the 0.5%Pd–B/PAL catalyst rapidly disappeared and deactivated after first cycle time. Thus, we mainly studied the stability of the 1% Pd–B/PAL catalyst. It can be seen that the 1%Pd–B/PAL catalyst still exhibited excellent catalytic performance and selectivity for the catalytic hydrogenation of o-CNB after three cycle times and the catalytic performance decreased and deactivated after four cycle times. The results might cause the loss of Pd–B amorphous alloy in the catalyst. The similar result was also observed in the platinum/PAL catalyst by Ma et al. [14]. The cause was further confirmed by the ICP-AES analysis on the recycled 1%Pd–B/PAL catalyst (listed in Table 1). The Pd content of Pd–B/PAL catalyst decreased from 0.97 to 0.21 wt% after fifth cycle time.

4. Conclusions: In summary, Pd–B/PAL amorphous catalyst was prepared by a simple chemical reduction method under mild condition by using PAL as support. PAL could reduce the electron density of Pd atoms because of the adsorption of its acid sites for electrons, resulting in the adsorption of Pd–B/PAL catalyst to nitro groups and the suppression on the hydrodechlorination of o-CNB. The Pd–B/PAL amorphous catalyst exhibited excellent catalytic performance and ultra-high selectivity (100%) for the hydrogenation of o-CNB to o-CAN under wide reaction conditions. The Pd–B/PAL amorphous catalyst also exhibited good stability and could be reused up to three times without the need to add the fresh catalyst.

6 References

[1] Wang C., Qiu J.S., Liang C.H., ET AL.: 'Carbon nanofiber supported Ni catalysts for the hydrogenation of chloronitrobenzenes', *Catal. Commun.*, 2008, **9**, pp. 1749–1753

[2] Cárdenas-Lizana F., Gómez-Quero S., Hugon A., ET AL.: 'Pd-promoted selective gas phase hydrogenation of *p*-chloronitrobenzene over alumina supported Au', *J. Catal.*, 2009, **262**, pp. 253–243

[3] Zhang X.J., Zhang P.P., Yu H.B., ET AL.: 'Mesoporous KIT-6 supported Pd-M$_x$O$_y$ (M=Ni, Co, Fe) catalyst with enhanced selectivity for *p*-chloronitrobenzene hydrogenation', *Catal. Lett.*, 2015, **145**, pp. 783–793

[4] Liu H.Q., Liang M.H., Xiao C.H., ET AL.: 'An excellent Pd-based nanocomposite catalyst for the selective hydrogenation of *para*-chloronitrobenzene', *J. Mol. Catal. A, Chem.*, 2009, **308**, pp. 79–86

[5] Kratky V., Kralik M., Mecarova M., ET AL.: 'Effect of catalyst and substituents on the hydrogenation of chloronitrobenzenes', *Appl. Catal. A, Gen.*, 2002, **235**, pp. 225–231

[6] Han X.X., Zhou R.X., Lai G.H., ET AL.: 'Influence of support and transition metal (Cr, Mn, Fe, Co, Ni and Cu) on the hydrogenation of *p*-chloronitrobenzene over supported platinum catalysts', *Catal. Today*, 2004, **93–95**, pp. 433–437

[7] Liu M.H., Bai Q., Xiao H.L., ET AL.: 'Selective hydrogenation of *o*-chloronitrobenzene over tin dioxide supported platinum-ruthenium bimetallic nanocatalysts without solvent', *Chem. Eng. J.*, 2013, **232**, pp. 89–95

[8] Ning J.B., Xu J., Liu J., ET AL.: 'A remarkable promoting effect of water addition on selective hydrogenation of *p*-chloronitrobenzene in ethanol', *Catal. Commun.*, 2007, **8**, pp. 1763–1766

[9] Xi C.Y., Cheng H.Y., Hao J.M., ET AL.: 'Hydrogenation of *o*-chloronitrobenzene to *o*-chloroaniline over Pd/C in supercritical carbon dioxide', *J. Mol. Catal. A, Chem.*, 2008, **282**, pp. 80–84

[10] Xu Q., Wang L., Chen J.R., ET AL.: 'Selective hydrogenation of *p*-chloronitrobenzene over Ru–Ir/γ-Al$_2$O$_3$ catalyst modified by organic amines', *Chin. J. Catal.*, 2007, **28**, pp. 579–581

[11] Xu Q., Liu X.M., Chen J.R., ET AL.: 'Modification mechanism of Sn^{4+} for hydrogenation of *p*-chloronitrobenzene over PVP-Pd/γ-Al$_2$O$_3$', *J. Mol. Catal. A, Chem.*, 2006, **260**, pp. 299–305

[12] Zhang J.L., Wang Y., Ji H., ET AL.: 'Magnetic nanocomposite catalysts with high activity and selectivity for selective hydrogenation of ortho-chloronitrobenzene', *J. Catal.*, 2005, **229**, pp. 114–118

[13] He D.P., Jiao X.D., Jiang P., ET AL.: 'An exceptionally active and selective Pt-Au/TiO$_2$ catalyst for hydrogenation of the nitro group in chloronitrobenzene', *Green Chem.*, 2012, **14**, pp. 111–116

[14] Ma H.W., Sun K.P., Li Y.W., ET AL.: 'Ultra-chemoselective hydrogenation of chloroanilines over HCl-acidified attapulgite-supported platinum catalyst with high activity', *Catal. Commun.*, 2009, **10**, pp. 1363–1366

[15] Sikhwivhilu L.M., Coville N.J., Pulimaddi B.M., ET AL.: 'Selective hydrogenation of *o*-chloronitrobenzene over palladium supported nanotubular titanium dioxide derived catalysts', *Catal. Commun.*, 2007, **8**, pp. 1999–2006

[16] Zhang Q.F., Su C., Cen J., ET AL.: 'The modification of diphenyl sulfide to Pd/C catalyst and its application in selective hydrogenation of *p*-chloronitrobenzene', *Chin. J. Chem. Eng.*, 2014, **22**, pp. 1111–1116

[17] Yu X.B., Wang M.H., Li H.X.: 'Study on the nitrobenzene hydrogenation over a Pd-B/SiO$_2$ amorphous catalyst', *Appl. Catal. A, Gen.*, 2000, **202**, pp. 17–22

[18] Ma Z.Y., Zhang L.X., Chen R.Z., ET AL.: 'Preparation of Pd-B/TiO$_2$ amorphous alloy catalysts and their performance on liquid-phase hydrogenation of *p*-nitrophenol', *Chem. Eng. J.*, 2008, **138**, pp. 517–522

[19] Zou J.J., Xiong Z.Q., Wang L., ET AL.: 'Preparation of Pd-B/γ-Al$_2$O$_3$ amorphous catalyst for the hydrogenation of tricyclopentadiene', *J. Mol. Catal. A, Chem.*, 2007, **271**, pp. 209–215

[20] Luo X.J., Yan X.H., Sun J.Q., ET AL.: 'Liquid-phase hydrogenation of *o*-chloronitrobenzene over Pd-B/Al$_2$O$_3$ amorphous alloy catalyst', *J. Chem. Eng. Chin. Univ.*, 2006, **20**, pp. 476–480

[21] Wang F., Zhang J., Liu C., ET AL.: 'Pd-palygorskite catalysts: preparation, characterization and catalytic performance for the oxidation of styrene', *Appl. Clay Sci.*, 2015, **105–106**, pp. 150–155

[22] Yang Z.W., Zhao X., Li T.J., ET AL.: 'Catalytic properties of palygorskite supported Ru and Pd for efficient oxidation of alcohols', *Catal. Commun.*, 2015, **65**, pp. 34–40

[23] Hou C.L., Yang H.M.: 'Preparation and enhanced photocatalytic activity of Pd-CuO/palygorskite nanocomposites', *Appl. Clay Sci.*, 2013, **74**, pp. 87–94

[24] Araújo Melo D.M., Ruiz J.A.C., Melo M.A.F., ET AL.: 'Preparation and characterization of Lanthanum palygorskite clays as acid catalysts', *J. Alloys Compd.*, 2002, **344**, pp. 352–355

[25] Wang C., Qiu J.S., Liang C.H.: 'Synthesis of carbon nanotubes-supported Pd/SnO$_2$ for the hydrogenation of *ortho*-chloronitrobenzene', *Chin. J. Catal.*, 2009, **30**, pp. 259–264